LIGO-P080124-00-Z

Searching for binary coalescences with inspiral templates: Detection and parameter estimation

Benjamin Farr[1,2], **Stephen Fairhurst**[1], **B.S. Sathyaprakash**[1]

[1] School of Physics and Astronomy, Cardiff University, The Parade, Cardiff, UK
[2] Department of Physics, Rochester Institute of Technology, 84 Lomb Memorial Drive, Rochester, NY 14623

Abstract. There has been remarkable progress in numerical relativity recently. This has led to the generation of gravitational waveform signals covering what has been traditionally termed the three phases of the coalescence of a compact binary - the inspiral, merger and ringdown. In this paper, we examine the usefulness of inspiral only templates for both detection and parameter estimation of the full coalescence waveforms generated by numerical relativity simulations. To this end, we deploy as search templates waveforms based on the effective one body waveforms extended to ringdown as well as standard post-Newtonian waveforms. We find that both of these are good for detection of signals but the parameter estimation is less impressive.

1. Introduction

Several ground-based interferometric detectors are now in operation to detect gravitational waves. These include the Laser Interferometric Gravitational-wave Observatory (LIGO) at two sites in Livingston and Hanford, USA, and the Virgo detector in Cascina, Italy. They have recently completed a first science run at or close to design sensitivity and are sensitive to gravitational waves from coalescing binaries at distances of tens to hundreds of megaparsecs depending on the total mass and the mass ratio of the system. The broadband sensitivity (40-400 Hz) of these detectors makes it possible to search for binaries with a rather large range of component masses from one to hundreds of solar masses. This range of masses includes both the neutron star binaries (which are known to exist) as well as neutron star-black hole and double black hole binaries (of which we have no observational evidence).

In this article we test the efficiency of inspiral waveforms for the detection and parameter estimation of the full coalescence signal. We restrict our attention to two waveform families. The first of the families is the Fourier domain model, called TaylorF2 or SPA [1], which is an analytical approximation to the Fourier transform of the standard post-Newtonian (PN) [2] waveform (i.e., TaylorT3) computed using the stationary phase approximation. The highest PN order available in the LIGO Scientific Collaboration (LSC) code base [3] for this family is $(v/c)^4$ (i.e. the second PN order). A number of searches by the LSC for compact binaries of low masses (i.e. $M < 25\,M_\odot$) have used this model as optimal templates [4, 5, 6, 7].

The second family we consider is the effective one-body (EOB) [8] model at three PN (i.e., $(v/c)^6$) order but terminated at the light ring. As discussed below, the EOB waveform is extends past the innermost stable circular orbit to the light ring, with the ringdown modes stitched to the end of the merger by a careful matching of the ringdown modes [9, 10, 11]. In this study, however, we use the EOB model without the ringdown modes. Thus, it captures some part of the coalescence signal, and is therefore better suited to search for higher mass signals. Here we will focus on the efficiency of our template bank to capture coalescence signals with the TaylorF2 and EOB models. In Section 2, we discuss in greater detail the dynamics of binary black hole mergers and the PN and EOB models.

We test the efficiency and parameter estimation accuracy of the searches in two different ways. First, in Section 3 we perform a Monte–Carlo study of the efficiency of the TaylorF2 and EOB models to detect the full waveforms. Since the full waveform is not known over the entire parameter space, we make use of the effective one body waveform extended, using numerical relativity results, to incorporate an accurate merger and ringdown. Then, in Section 4, we perform a similar comparison making use of waveforms generated numerically. This study was performed on the NINJA [12] data set which comprised simulated data for the LIGO and Virgo detectors with numerically obtained binary coalescence signals added.

2. Binary black hole dynamics

The evolution of a black hole binary is driven by back-reaction due to the emission of gravitational waves which causes the system to inspiral and merge. Confident detection of the emitted signal is greatly facilitated by an accurate understanding of the dynamics of the binary and the shape of the emitted waveform during inspiral and merger. The early evolution of a binary can be well-modelled by the PN approximation during which the system slowly inspirals on an adiabatic sequence of quasi-circular orbits located at the (stable) minimum of the changing effective potential. In fact,

for most of its lifetime a binary black hole can be accurately described by the balance of the rate of change of the binding energy with the energy carried away to infinity by the radiation as given by the quadrupole formula.

As the system evolves, the effective potential changes and there reaches a point when the potential transforms from one having a stable minimum and an unstable maximum to one having just an unstable minimum. After this, the system no longer possesses any bound orbits. The transition point, called the last stable orbit (LSO), occurs when the radius r of the orbit (in Schwarzschild coordinates) approaches $r = 6GM/c^2$, where M is the total mass of the system. In terms of the dominant component of the emitted radiation, this corresponds to a gravitational-wave frequency of $f_{\rm insp} \simeq 440\,{\rm Hz}(M/10M_\odot)^{-1}$. Therefore, For masses less than about $10\,M_\odot$, only the inspiral stage of the coalescence lies in the detector's sensitive band of 40-400 Hz.

Once the system passes the LSO, the two black holes plunge towards each other and merge in about one orbital time scale of the LSO to form one single distorted black hole. This is the so-called merger phase which is amenable to analytic description by a clever re-summation of the PN approximation but more recently numerical relativity simulations have provided a better understanding of the merger phase and continue to provide new insights. The frequency of the waves during this phase changes rapidly from $f_{\rm merge} \simeq 440\,{\rm Hz}(M/10\,M_\odot)^{-1}$ to $1200\,{\rm Hz}\,(M/10\,M_\odot)^{-1}$. During the late stages of the coalescence, the highly distorted black hole, that results from the merger of the two parent black holes, settles down to an axi-symmetric quiescent state by emitting its deformation in the form of gravitational waves. The radiation from this phase is well described by black hole perturbation theory and consists of a set of quasi-normal modes (often referred to as ringdown signal) whose fundamental frequency is $f_{\rm ring} \sim 1800\,(M/10\,M_\odot)^{-1}$ when two equal mass non-spinning black holes merge to form a single black hole whose spin magnitude is estimated to be $J/M^2 \simeq 0.7$. The first two overtones of this mode have frequencies of $\sim 1650\,{\rm Hz}$ and $\sim 1700\,{\rm Hz}$, for the same system.

2.1. Search templates

The foregoing discussion hints that binaries whose total mass is less than about $10\,M_\odot$ can be detected by using templates that are described by the PN approximation. In fact, experience suggests that we could make do with the PN waveform as templates even when the total mass is as large as about $25\,M_\odot$ and they have been used in the search for low-mass systems (i.e. systems with their total mass less than about $25M_\odot$) in the data from LIGO and Virgo. However, for higher mass black hole binaries (i.e. binaries with their total mass greater than about $25M_\odot$) the merger of the binary occurs in the detector's sensitive band. At merger, the dynamics is no longer adiabatic and is, therefore, not well-modelled by PN expansion. It has been a long standing aim of numerical relativity to generate the full waveforms for gravitational wave detection from higher mass black holes.

There has been significant progress recently in numerical relativity with several groups having successfully simulated the merger of two black holes [13, 14, 15]. The longest of these simulations last for tens of orbits [16], and they cover different mass ratios and are beginning to expore the space of component masses with spins.

Nearly a decade ago, analytical work by Buonanno and Damour [8] extended the PN dynamics beyond the last stable orbit to calculate the merger dynamics. This analytical method, called EOB computes the dynamics up to light ring of the effective potential and the waveform can be computed for separations larger than about $r \simeq 2.2\,M$. In this work we have used the EOB waveform

terminated at the light ring as search templates. The EOB formalism indeed proposes that the end of this merger phase be completed by matching the amplitude of the waveform and its derivaties to the ringdown signal (namely, the various modes and their overtones). Moreover, the availability of numerical relativity simulations has helped in fixing certain unknown higher order (4PN) terms in the EOB model by fitting the analytical waveform to numerical relativity. Current implementation of this proposal includes the fundamental mode and two of its overtones to match the value and the first two derivatives and this called the EOBNR model which was also used in the NINJA project [12]. EOBNR will be used to calibrate the efficiency of the inspiral models used in this study.

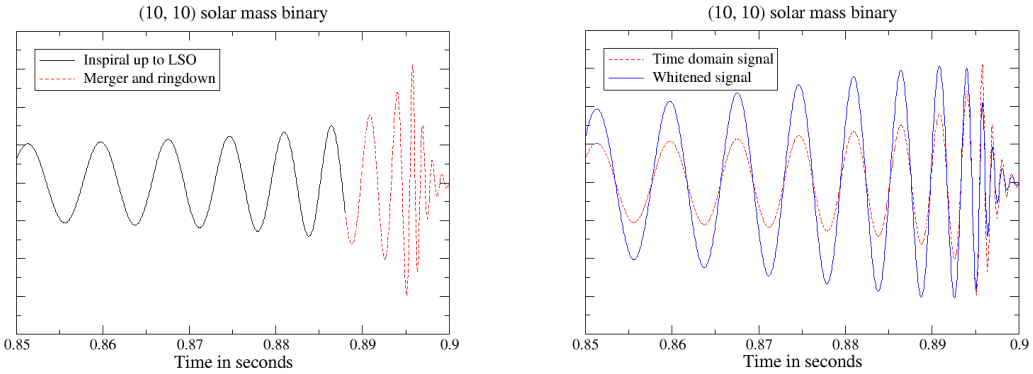

Figure 1. An example of the EOBNR waveform for a binary consisting of two equal mass black holes each $10\,M_{\odot}$. The EOB dynamics allows the computation of the inspiral (left panel, black solid line) and merger phases (left panel, roughly the first two cycles of the red dashed line) but the ringdown (left panel, latter part of the red dashed line) is stitched to the end of the merger phase by matching the amplitude of the waveform and its first two derivatives by using the fundamental quasi-normal mode and its first two overtones. The right panel compares the time-domain signal (red dashed line) with the whitened signal (blue solid line).

More recently, Ajith et al [17, 18] have used a phenomenological approach to match the inspiral phase from PN approximation to the merger and ringdown from numerical relativity. Here, the inspiral stage of the waveform is based upon the standard PN expansion. The merger and ringdown are modelled phenomenologically and the parameters are fitted using input from numerical relativity waveforms. In the long run, it is likely that these full waveforms will be used as templates for searching for inspiral waveforms in gravitational wave detectors. At present, however, the waveforms describing the full signal, particularly in the spinning case are still under development.

In order to test the efficiency of EOB and TaylorF2 families, we will use the EOBNR waveform as our "true" waveform and see how well these partial waveforms perform in both detection and parameter estimation.

2.2. An example waveform

Fig. 1 shows the waveform expected from a pair of $10\,M_{\odot}$ black holes during the last 50 ms before merger. The left panel shows the time-domain waveform $h(t)$ and the right panel compares the time-domain waveform with the signal how the initial LIGO detector (whose noise has been whitened)

perceives the signal in the time-domain. In other words, the right panel plots whitened template $q(t)$ given by

$$q(t) = \int_{-\infty}^{\infty} \frac{H(f)}{\sqrt{S_h(f)}} \exp(-2\pi i f t)\, \mathrm{d}f,$$

where $H(f) = \int_{-\infty}^{\infty} h(t) \exp(2\pi i f t)\, \mathrm{d}t$ is the Fourier transform of the time-domain signal and $S_h(f)$ is the one-sided noise power spectral density of initial LIGO. In the left panel, the inspiral part of the signal given EOB dynamics is shown in black solid line followed by the merger and ringdown phases in red dashed line. The right panel compares the time-domain waveform in the left panel (red dashed line) with the whitened signal (blue solid line).

Note that although the time-domain signal is dominated by the merger and the ringdown phases, the detector noise spectral density (i.e, $S_h(f)$) supresses them, making the inspiral phase more dominant. For systems with greater masses, more of the merger phase appears in band. For systems with total mass larger than about $80\,M_\odot$ the merger and ringdown signals begin to dominate over the inspiral phase. For such systems it is important to deploy EOBNR templates. As a result, we cannot expect our template families to do well for high mass binaries.

3. Bank Efficiency

Matched filtering, the data analysis technique used in most searches for binary black holes, is pretty sensitive to the phasing of the signal, which in turn depends on (a subset of) the source parameters. In the case of non-spinning black holes on a quasi-circular orbit, the only parameters that we must consider are the two masses. The location of the binary on the sky, the distance to the source, the polarization of the wave, etc., are not important for a single detector as they simply affect the amplitude of the waveform. Although we won't know the time at which the binary merges nor the phase of the signal at that epoch, these parameters need not be explicitly searched for [19], and are easily extracted in the process of maximising the cross-correlation of the template with the data.

3.1. Template bank

Our goal in this Section is to study the efficiency of the two template families in detecting binary black hole coalescences. To this end we first set up a template bank – a set of points in the parameter space of the component masses. A geometric algorithm described by Babak et al [20] is used to generate the template bank and it is the same algorithm irrespective of which family of waveforms is used to filter the signals. However, the range of masses is different for the two families. In the case of TaylorF2 we set up a template bank with the total mass in the range $[10,\, 35]\,M_\odot$ and a mimimum component mass of $5\,M_\odot$. The upper limit of the range is dictated by the fact that the TaylorF2 model is not a good approximation for detection beyond about $\sim 25\,M_\odot$. A slightly larger value of $35\,M_\odot$ cures any ill effects of a discrete boundary in the parameter space. For the EOB family we use a larger range of $[10,\, 70]\,M_\odot$ for the total mass but the same minimum value of $5\,M_\odot$ for component masses.

In addition to the range of the component masses, our template bank algorithm requires us to specify a parameter called the *minimal match,* MM. The mimimal match is the smallest overlap guaranteed between a signal with random source parameters and the template nearest (in the geometrical sense) to it in the parameter space. Assumptions made in the construction of the template placement algorithm imply that this will be strictly true only when (a) the templates and signals belong to the same family, and (b) the ending frequency (i.e., the LSO, the light ring or

the ringdown mode, depending on the waveform in question) is greater than the upper end of the sensitivity band. The latter condition further implies that we can hope to achieve overlaps of MM or greater only for waveforms whose total mass is smaller than a certain value depending on the detector bandwidth; in the case of initial LIGO this $10\,M_\odot$. We have chosen $MM = 0.97$, but we cannot expect to achieve this overlap for total mass less than $10\,M_\odot$ since our templates and signals belong different PN approximations. The template placement algorithm chooses a hexagonal grid in the two-dimensional parameter space of the component masses and it is an optimal algorithm in the sense that it gives the smallest number of templates possible for a given mimimal match [21].

Having constructed a template bank we then generate an EOBNR signal with the values of its masses and the epoch of and the phase at coalescence, all chosen randomly but in a given range. Since the EOBNR extends beyond the LSO, it is possible to generate signals with the total mass in the range $[10,\, 300]\,M_\odot$ and minimum component mass of $5\,M_\odot$.

Next, for each point in the template bank we generate waveforms from our tempalte families (EOB and TaylorF2) and measure their overlap with the random signal. The overlap $\mathcal{O}_k$ of the kth template $q_k(t;\, m_1^k,\, m_2^k)$ and the signal $h(t)$ is defined by

$$\mathcal{O}_k(t;\, m_1^k,\, m_2^k) = 2\int_{f_l}^{f_u} \left[H(f)Q_k^*(f;\, m_1^k,\, m_2^k) + H^*(f)Q_k(f;\, m_1^k,\, m_2^k)\right]\, e^{-2\pi i f t}\, \frac{\mathrm{d}f}{S_h(f)},$$

where $H(f)$ and $Q(f)$ are the Fourier transforms of $h(t)$ and $q(t)$, respectively, and Q^* is the complex conjugate of Q. This allows us to compute the maximum overlap between our template waveforms and a random signal‡. This process is repeated for 1,000 different realizations of the random mass parameters and the maximum of the overlap over the entire template bank is recorded in each case. We will now discuss the results of these simulations.

3.2. Efficiency for detection

Fig. 2 plots the results of our simulation. The left panel shows the (maximum) overlaps of the TaylorF2 template bank with random signals, one dot for each trial. The right panel shows the same but for the EOB template bank. The TaylorF2 model has overlaps larger than 90% for only signals whose total mass is less than about $22\,M_\odot$. The overlap falls of quickly for masses larger than this, reaching slightly more than 0.5 when the total mass is about $50\,M_\odot$. The fact that the overlap remains unchanged beyond $50\,M_\odot$ is probably some spurious effect.

In contrast, the EOB model seems to achieve overlaps of better than 85% for systems whose total mass is less than $150\,M_\odot$, and the overlaps remain more than 65% even for systems with total mass less than $200\,M_\odot$. The oscillatory behaviour seen in this case is due to an edge effect: the density of templates gets smaller and smaller as the total mass becomes larger. There are only a handful of templates between say a template mass of $50\,M_\odot$ and $70\,M_\odot$. As a result, a single template might be available for a pretty large range of masses, causing the overlaps to swing up and down as the total mass is increased.

The most striking aspect of our simulation is that although the EOB template bank extends only up to $70\,M_\odot$, the model seems to capture the EOBNR signals all the way up to $300M_\odot$, with overlaps better than 65%. There are two ways in which this could happen. It is possible that the very high mass EOB signals are very short in the detector band (perhaps a cycle or two) and the abrupt cutoff of the template as a result of termination at the light ring could bleed power into a

‡ For the sake of saving space we have not discussed the maximization over the phase of the signal. This can be found, for instance, in Ref. [19].

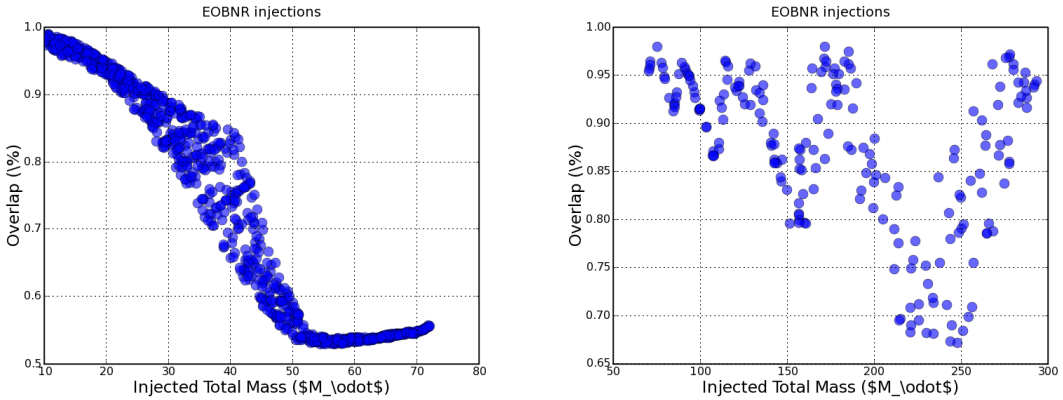

Figure 2. These plots depict of the efficiency of the TaylorF2 (left panel) and EOB (right panel) template banks in detecting the coalescence waveforms assumed to be well-represented by EOBNR. Each dot corresponds to the overlap of a random EOBNR signal maximized over the template bank consisting of TaylorF2 and EOB waveforms.

frequency region where there is no power in reality§. This spurious template power may lead to large overlaps with higher mass EOBNR waveforms that have their real power at these frequencies. For instance, an EOB waveform for a (50, 50) $M_\odot$ binary terminated at the light ring will not have any real signal power in the frequency range 120-200 Hz. However, the abrupt cutoff of the signal at 120 Hz (the frequency of gravitational waves at the light ring for this system) will bleed power in the above range. Now, the EOBNR has its peak signal power precisely in this very frequency range. Therefore, an abrupt termination can cause a spuriously large overlaps between our template and the random EOBNR signals.

Large overlaps between an EOB template and a high-mass EOBNR signal could also arise due to an accidental match between the low-frequency inspiral part of an EOB waveform with the high-frequency merger and ringdown part of the EOBNR signal. We believe this is the reason for good overlaps of the EOB templates with the large majority of the EOBNR signals with masses larger than about 150 $M_\odot$. However, a significant number of high-mass EOBNR signals end up having a good overlap due to spurious signal power in detector band.

TaylorF2 does not suffer from this predicament. This is because TaylorF2 is generated in the Fourier domain and the abrupt cutoff of the signal does not cause any problem in the frequency domain and we are unconcerned with spurious effects in the time-domian as they occur outside the region of our interest. We shall see in the next Section that as a result, the estimation parameters is comparatively better in the case of TaylorF2 than EOB terminated at the light ring.

3.3. Efficiency for parameter estimation

Match filtering statistic gives the likelihood for a signal to be present in the data as opposed to the data being pure background noise. The parameters of the template which maximize the likelihood

§ The spurious power is in itself not a bad thing but large noise glitches in the region where there is spurious power could cause false alarms. This is especially the case when the detector noise is contaminated by large amplitude non-stationary noise glitches.

are maximum likelihood estimates. Having determined the efficiency of our template banks in capturing the coalescence signals, we next consider how good they are in measuring the signal parameters in the maximum likelihood sense. If the template waveforms and the signal they are intended to detect both belong to the same family then in the limit of large signal-to-noise ratio the distribution of the maximum likelihood estimates will be centred on the true signal parameters. We are in a situation wherein the template waveforms and the signals they are intended to recover belong to different approximations. Therefore, one can expect a systematic bias in the estimation of parameters.

To gauge the reliability of the two families in estimating the parameters of the true signal we make use of the results of the simulation from the previous Section. This simulation computed the overlap of the templates with the signals in the absence of any noise. Therefore, the parameters of templates that maximized the overlap when compared to the true parameters of the EOBNR signal give a measure of the systematic bias in parameter estimation due to the difference in the waveform families representing the templates and the signal. Fig. 3 are 3D plots showing the measured total mass of the template (y-axis) vs the true total mass of the EOBNR signal (x-axis) and the corresponding overlap (indicated by colour coding). The left panel is for the TaylorF2 model and the right for the EOB.

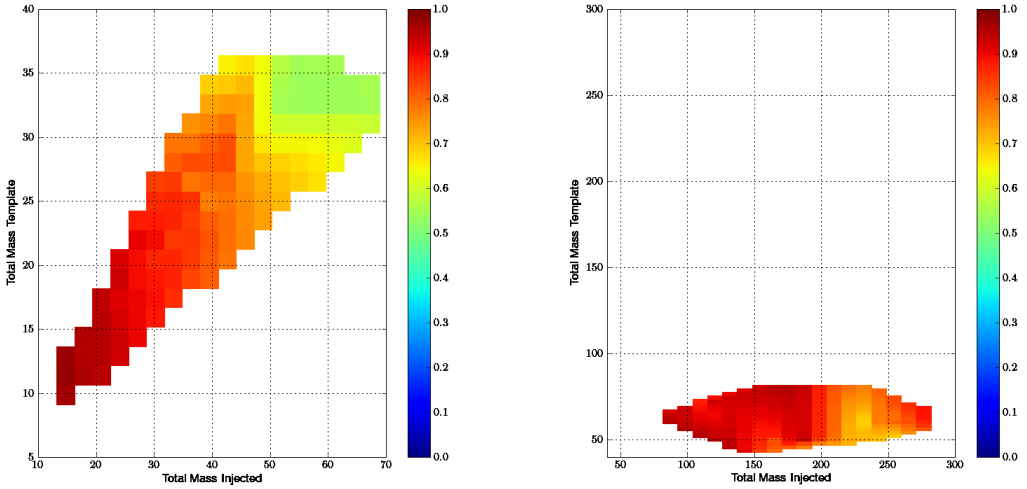

Figure 3. Parameter estimation accuracies for the TaylorF2 (left panel) and the EOB (right panel) models. The total mass of the injected EOBNR signal is plotted vs the total mass of the template that obtained the best overlap. The overlap itself is shown as a colour map. Clearly, there is a positive correlation between the injected and measured masses in the case of TaylorF2 model, with the spread in the measured values becoming larger at higher masses which, as expected, correspond to smaller overlaps. EOB model has pretty poor measurement accuracy.

First, note that the range of total mass explored by the two models is significantly different. TaylorF2 simulation had its template bank in the range $[10, 35]\,M_\odot$ while for EOB the range was $[10, 70]\,M_\odot$. EOBNR injections were in the range $[10, 70]\,M_\odot$ and $[10, 300]\,M_\odot$, in the case

of TaylorF2 and EOB simulations, respectively. It is immediately clear from Fig. 3 that of the two models used in this study, TaylorF2 is vastly superior in parameter measurement although its detection efficiency was rather poor compared to EOB. However, there is noticeable bias in the estimation of the total mass. A reasonable guess for the measured total mass $M_{\rm det}$ when the injected total mass is $M_{\rm inj}$ is given by $M_{\rm det} = \frac{1}{2}M_{\rm inj} + 5M_{\odot}$. For systems whose true total mass is larger (smaller) than $\sim 10\,M_{\odot}$ the measured total mass is under-estimated (over-estimated). The fluctuation in the total mass is larger for greater mass templates but this is hardly a surprize as parameter estimation is known to become poorer at higher end of the mass range.

In the case of EOB, there is hardly any correlation between the measured and true parameters. As discussed in Sec. 3.2 large overlaps between an EOB template and a high-mass EOBNR signal could arise due to an accidental match between the low-frequency inspiral part of an EOB waveform with the high-frequency merger and ringdown part of the EOBNR signal. Consequently, although the EOB model has better efficiency for detection it is bound to suffer from poor estimation of parameters. We suspect this is the reason for the lack of correlation between injected and measured total mass for a large majority of the EOBNR signals. Additionally, since the EOB model is abrutly terminated at the light ring, a significant number of high-mass EOBNR signals end up having a good overlap with the "wrong" EOB template as a result of the latter's spurious in band power. This is a serious predicament for the EOB model. In fact, the detection efficiency of EOB could be worse than TaylorF2 if one were to apply a signal-based veto such as the χ^2-veto which tests for the goodness of fit between the template and the signal in the frequency domain [22].

4. NINJA Results

The Numerical INJection Analysis (NINJA) project was a mock data challenge, where the data were generated at the design sensitivity of the initial LIGO and Virgo detectors and numerical relativity waveforms provided by a number of groups were added to the data. A number of data analysis methods were applied to the data, and the results of the NINJA project are available elsewhere [12]. For the NINJA analysis, we performed several runs through the data using the LSC's Compact Binary Coalescence (CBC) analysis pipeline. Here, we restrict our attention to two runs through the data which are similar to the TaylorF2 and EOB analyses described in the previous section. This allows us to investigate the issues of detection and parameter estimation using these templates to search for full waveforms obtained from numerical relativity. The results are similar to those obtained in the previous section, namely that the EOB search has a greater efficiency than the TaylorF2 search, but that both can detect high mass signals, although the parameter estimation is poor.

The CBC pipeline was designed to analyze data from a network of detectors to search specifically for gravitational wave signals from binary neutron stars and black holes [6]. It proceeds as follows: First, a bank of templates covering the desired mass range is produced. For the NINJA analysis we used a template bank covering masses between 20 and $90M_{\odot}$ with a minimal match of 0.97. The data from each of the detectors is separately match filtered against the template waveforms [23]. For this analysis, we restricted attention to the mock data generated for the three LIGO detectors (the 4km and 2km detectors denoted H1 and H2 respectively at Hanford, WA and the 4km L1 detector at Livingston, LA). A trigger is produced whenever the signal to noise ratio exceeds the desired threshold of 5.5. A coincident trigger is recorded whenever there are triggers from two or more detectors with comparable masses and coalescence times [24]. Finally, these coincident triggers are subjected to a set of signal based vetoes, in particular the χ^2 [22] and r^2 [25]

Template	TaylorF2	EOB
Freq. Cutoff	LSO	Light Ring
PN Order	2 pN	2 pN
Found Inj, Single Detector (H1, H2, L1)	72, 43, 66	91, 64, 82
Found Inj, Coincidence	59	83
Found Inj, Coincidence + Signal Vetoes	59	80

Table 1. Results of inspiral search for NINJA waveforms. There were 160 injections performed into the data. The table above shows the number of injections which were recovered using the two waveform families. The EOB search shows a significantly higher sensitivity than the TaylorF2 waveforms evolved to LSO. Note that virtually all simulations which passes the initial coincidence requirement also survived the signal consistency checks.

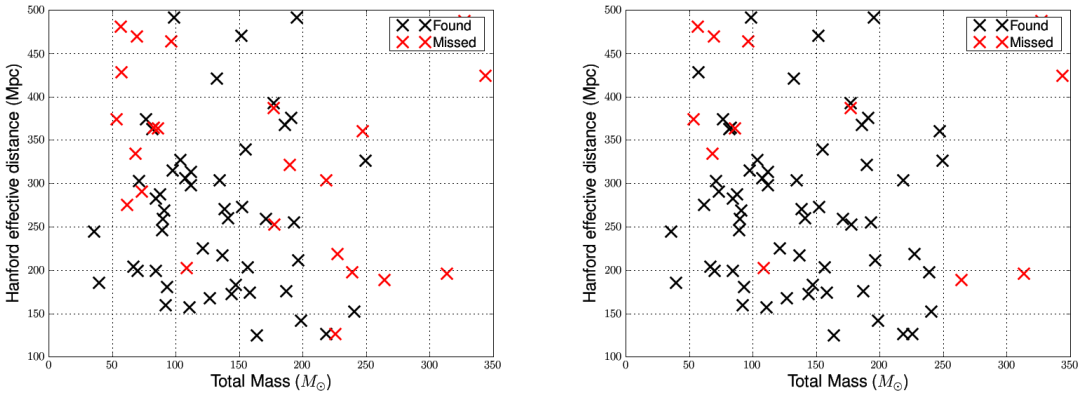

Figure 4. Found and missed numerical injections for the TaylorF2 (left panel) and EOB (right panel) searches of the NINJA data. The found and missed injections are plotted on the total mass, Hanford effective distance plane. The effective distance for a detector provides a measure of the amplitude of the signal at that site, taking into account the distance and orientation of the source. For both searches, the majority of the close simulations are recovered. EOB templates are seen to perform better, particularly at higher masses.

tests, designed to separate signals from non-stationary transients in the noise.

Our results are summarized in Table 1 which shows the number of injections recovered by the analysis pipeline at each stage of the analysis for the two searches described here. The EOB search is capable of detecting a greater fraction of the simulated signals than the TaylorF2 templates truncated at LSO. This is further highlighted in Figure 4 where we show those simulated signals which were recovered by the two different waveform families. The EOB model clearly performs better, particularly at higher masses. This is consistent with the findings of the previous section.

Next, we turn to parameter estimation. Figure 5 shows the accuracy with which the total mass of the simulated signals is recovered using the inspiral only waveforms. For both the TaylorF2 and EOB models, the parameter recovery is poor, particularly at higher masses. This is to be expected, since we are searching with partial waveforms and, at the higher masses, it is the merger and ringdown of the simulations which occupies the sensitive band of the detectors.

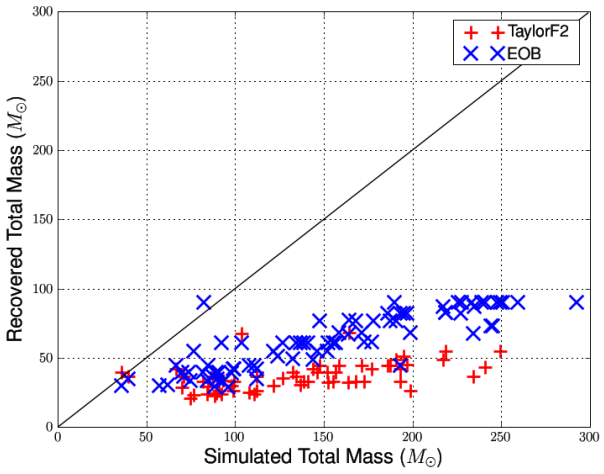

Figure 5. Accuracy of recovering the total mass of simulated signals for the TaylorF2 (red +) and EOB (blue ×) models. For both of the searches, the total mass is estimated poorly and systematically lower than the simulated mass. This is due to the fact that the search has been performed with inspiral only waveforms for which the search extends only up to $90M_\odot$.

5. Discussion

In the coming years, the first detection of gravitational waves from coalescing binaries will surely be achieved. Following the first detection, attention will focus on extracting as much astrophysical information as possible from the observed signal. In the studies described here, we have addressed the ability to perform both the detection and parameter estimation problems using template waveforms which cover only part of the binary coalescence. We have made use of two different waveforms — the TaylorF2 PN waveforms taken to LSO and the EOB waveforms to light ring. In addition, we have used two different methods to evaluate the detection and parameter estimation capabilities of these signals — a Monte–Carlo study using EOBNR waveforms as the "true" signal, and an analysis of numerical relativity waveforms in the NINJA data. In all cases, the conclusion is the same: the inspiral only templates are useful for detection of the signal, but do not provide good parameter estimation, particularly for the higher mass signals. This is to be expected as, for high mass binaries, it is the merger and/or ringdown which occurs at the most sensitive frequency of the detectors. We observe that the EOB waveforms perform somewhat better than the TaylorF2 waveforms, and conclude that this is based upon two effects. The EOB waveforms extend to a higher frequency and can therefore catch part of the merger signal. Additionally, they terminate abruptly in the time domain which leads to spurious power at higher frequencies being present in the template.

The results of this study show that post-Newtonian based inspiral only waveforms will not be sufficient for satisfactory detection and parameter estimation of higher mass black hole binaries. Full waveforms derived from a synthesis of post-Newtonian waveforms and numerical relativity results, such as the EOBNR model [26], or phenomenological models, such as [17, 18], will be necessary.

References

[1] Droz S, Knapp D J, Poisson E and Owen B J 1999 *Phys. Rev. D* **59** 124016 (*Preprint* gr-qc/9901076)
[2] Blanchet L 2002 *Living Rev. Rel.* **5** 3 (*Preprint* gr-qc/0202016)
[3] Lsc algorithm library URL http://www.lsc-group.phys.uwm.edu/lal
[4] Abbott B *et al.* (LIGO Scientific) 2004 *Phys. Rev. D* **69** 122001 (*Preprint* gr-qc/0308069)
[5] Abbott B *et al.* (LIGO Scientific) 2005 *Phys. Rev.* **D72** 082001 URL http://arxiv.org/abs/gr-qc/0505041
[6] Abbott B *et al.* (LIGO Scientific) 2008 *Phys. Rev. D* **77** 062002 (*Preprint* 0704.3368)
[7] Abbott B *et al.* (LIGO Scientific) 2008 Search for gravitational waves from low-mass binary coalescences in the first calendar year of s5 ligo data in preparation
[8] Buonanno A and Damour T 1999 *Phys. Rev. D* **59** 084006 (*Preprint* gr-qc/9811091)
[9] Damour T and Nagar A 2008 *Phys. Rev. D* **77** 024043 (*Preprint* 0711.2628)
[10] Damour T, Nagar A, Dorband E N, Pollney D and Rezzolla L 2008 *Phys. Rev. D* **77** 084017 (*Preprint* 0712.3003)
[11] Damour T, Nagar A, Hannam M, Husa S and Bruegmann B 2008 *Phys. Rev. D* **78** 044039 (*Preprint* 0803.3162)
[12] Collaboration N *In preparation*
[13] Pretorius F 2005 *Phys. Rev. Lett.* **95** 121101 (*Preprint* gr-qc/0507014)
[14] Campanelli M, Lousto C O, Marronetti P and Zlochower Y 2006 *Phys. Rev. Lett.* **96** 111101 (*Preprint* gr-qc/0511048)
[15] Baker J G, Centrella J, Choi D I, Koppitz M and van Meter J 2006 *Phys. Rev. Lett.* **96** 111102 (*Preprint* gr-qc/0511103)
[16] Boyle M *et al.* 2007 *Phys. Rev. D* **76** 124038 (*Preprint* 0710.0158)
[17] Ajith P *et al.* 2008 *Phys. Rev. D* **77** 104017 (*Preprint* 0710.2335)
[18] Ajith P *et al.* 2007 *Class. Quant. Grav.* **24** S689–S700 (*Preprint* 0704.3764)
[19] Sathyaprakash B and Dhurandhar S 1991 *Phys. Rev. D* **44** 3819–3834
[20] Babak S, Balasubramanian R, Churches D, Cokelaer T and Sathyaprakash B S 2006 *Class. Quant. Grav.* **23** 5477–5504 (*Preprint* gr-qc/0604037)
[21] Cokelaer T 2007 *Phys. Rev. D* **76** 102004 (*Preprint* 0706.4437)
[22] Allen B 2005 *Phys. Rev. D* **71** 062001 (*Preprint* gr-qc/0405045)
[23] Allen B, Anderson W G, Brady P R, Brown D A and Creighton J D E 2005 FINDCHIRP: An algorithm for detection of gravitational waves from inspiraling compact binaries (*Preprint* gr-qc/0509116)
[24] Robinson C A K, Sathyaprakash B S and Sengupta A S 2008 A geometric algorithm for efficient coincident detection of gravitational waves (*Preprint* 0804.4816)
[25] Rodríguez A 2007 *Reducing false alarms in searches for gravitational waves from coalescing binary systems* Master's thesis Louisiana State University URL http://www.ligo.caltech.edu/docs/P/P070056-00.pdf
[26] Buonanno A *et al.* 2007 *Phys. Rev. D* **76** 104049 (*Preprint* 0706.3732)